Small-Scale Spatial Heterogeneity of Photosynthetic Fluorescence Associated with Biological Soil Crust Succession in the Tengger Desert, China

Lan, Shubin; Thomas, Andrew; Tooth, Stephen; Wu, Li; Hu, Chunxiang

Published in:
Microbial Ecology

DOI:
10.1007/s00248-019-01356-0

Publication date:
2019

Citation for published version (APA):
Lan, S., Thomas, A., Tooth, S., Wu, L., & Hu, C. (2019). Small-Scale Spatial Heterogeneity of Photosynthetic Fluorescence Associated with Biological Soil Crust Succession in the Tengger Desert, China. *Microbial Ecology*, *78*, 936-948. https://doi.org/10.1007/s00248-019-01356-0

Small-scale spatial heterogeneity of photosynthetic fluorescence associated with biological soil crust succession in the Tengger Desert, China

Shubin Lan[1,2], Andrew David Thomas[2], Stephen Tooth[2], Li Wu[2,3], Chunxiang Hu[1]*

[1] Key Laboratory of Algal Biology, Institute of Hydrobiology, Chinese Academy of Sciences, Wuhan, 430072, China

[2] Department of Geography and Earth Sciences, Aberystwyth University, Aberystwyth, SY23 3DB, UK

[3] School of Resources and Environmental Engineering, Wuhan University of Technology, Wuhan, 430072, China

∗ Corresponding author: Tel/Fax.: +86 27 68780866; E-mail address: cxhu@ihb.ac.cn (C.X. Hu)

Abstract: In dryland regions, biological soil crusts (BSCs) have numerous important ecosystem functions. Crust species and functions are, however, highly spatially heterogeneous and remain poorly understood at a range of scales. In this study, chlorophyll fluorescence imaging was used to quantify millimeter-scale patterns in the distribution and activity of photosynthetic organisms in BSCs of different successional stages(cyanobacterial, lichen, moss three main successional stages and three intermix transitional stages) from the Tengger Desert, China. Chlorophyll fluorescence images derived from the Imaging PAM (Pulse Amplitude Modulation) showed that photosynthetic efficiency (including the maximum and effective photosynthetic efficiency, respectively) and fluorescence coverage is significantly different (P<0.05) between cyanobacterial, lichen and moss crusts, and that increasing photosynthetically active radiation (PAR) reduced the effective photosynthetic efficiency (Yield). The distribution of photosynthetic organisms in crusts determined Fv/Fm (ratio of variable fluorescence to maximum fluorescence) frequency pattern, although the photosynthetic heterogeneity (*SHI* index) was not significantly different (P>0.05) between cyanobacterial and moss crusts, and showed a unimodal pattern of Fv/Fm values. In contrast, photosynthetic heterogeneity was significantly higher (P<0.05) in lichen, cyanobacteria-moss and lichen-moss crusts, with a bimodal pattern of Fv/Fm values. Point pattern analysis showed that the distribution pattern of chlorophyll fluorescence varied at different spatial scales and also among the different crust types. These new results provide a detailed (millimeter-scale) insight into crust photosynthetic mechanisms and spatial distribution patterns in different crust types. Collectively, this information provides an improved theoretical basis for crust maintenance and management in dryland regions.

Keywords: Drylands; biological soil crusts; chlorophyll fluorescence; photosynthesis; heterogeneity; Succession

Introduction

Biological soil crusts (BSCs) are widely distributed in dryland regions, and can comprise more than 70% of the living cover in some areas [1, 2]. Within the uppermost millimeters of the soil surface, cyanobacteria, algae, heterotrophic bacteria and micro-fungi cement and bind soil particles to form a complex mosaic BSC layer which exists at the interface of the soil and atmosphere, and thus regulates surface boundary conditions in dryland regions. [3-6]. BSCs play several important roles, which include: i) facilitating soil surface stabilization, fertility and microbial diversity [6-8]; ii) influencing porosity, infiltration and the distribution of water in the soil profile [4, 9, 10]; iii) affecting the process of germination and growth of vascular plants [11]; and iv) providing food and habitat for a variety of soil fauna [12].

Heterogeneity is the degree of variation and complexity of processes and patterns in time and space, and is one of the inherent properties of many ecological phenomena [13-15]. It is, however, scale dependent, and the same phenomenon and process when viewed at different scales, may differ significantly [13, 16, 17]. Temporally, different dominant species of photosynthetic organisms appear at different times in the process of BSC succession. Based on the dominant coverage of photosynthetic organisms, BSCs are usually categorized into cyanobacterial crusts (or microalgal or algal crusts), lichen crusts and moss crusts, representing the three main successional stages [2, 4]. Generally, cyanobacterial crusts are the first to form due to the ability of the filamentous cyanobacteria to colonize soil, and so normally represent the early stage of BSCs [3, 18]. Given the right conditions, these crusts can gradually develop and succeed to lichen- and moss-dominated crusts [2, 6, 19-21]. However, in addition to the three main successional stages, there are transitional BSC types and many alternative development scenarios such as cyanobacteria-lichen crusts, cyanobacteria-moss crusts, and lichen-moss crusts [4].

At the largest scale, the heterogeneity of BSCs is predominantly controlled by climatic variables, such

as temperature and precipitation [22]. At a landscape scale, for instance, climate, geomorphology and biota interact to determine soil physiochemical characteristics, such as soil pH, trace elements and water content, which affect the distribution and succession of BSCs [2, 23, 24]. At the finer patch scale, the characteristics and controls of crust heterogeneity remain poorly understood, although it has been reported that there is a small-scale vertical heterogeneity in BSCs. This vertical heterogeneity may include stratification and physiochemical gradients through the vertical profile of BSCs, with rapid changes in light intensity, pH and oxygen concentration occurring over the millimeter range [4, 5, 23, 25].

In dryland regions, BSCs are dry most of the time and therefore they are not metabolically active [21, 26]. For instance, in the Tengger desert, it has been found the dominant photosynthetic species (cyanobacteria) are mainly distributed inside the early successional cyanobacterial crust substrate, while in later successional BSCs, the dominant lichens and mosses are directly distributed on the soil surface [26]. Consequently, the later successional BSCs are more readily able to use water, even during very small precipitation events [27, 28]. In addition, it has been found that later successional crusts have higher carbon fixation efficiency than early successional ones [26]. In drylands research more generally, there has been increasing interest in photosynthesis and the relative ecological functions of BSCs, but so far most crust samples have been studied in bulk at a relatively coarse (centimeter and upwards) scale. Research is needed at a finer (mm) scale to evaluate the photosynthetic heterogeneity in BSCs and to investigate variations in photosynthetic mechanisms and responses associated with BSC succession.

In short, while there has been considerable work in drylands to investigat the influence of heterogeneity and associated resource gradients at large spatial scales (e.g. [29]) and at plant-patch scales (e.g. [30]), there has been limited investigation into variations *within* small BSC patches. Studying heterogeneity at this spatial scale is important because the distribution pattern of photosynthetic organisms

89 in BSCs provides greater insight into crust photosynthetic mechanisms, improves the accuracy of
90 discriminating crust successional stages, and provides an opportunity to establish links between spatial
91 heterogeneity and ecological relevance at a fine scale. Against this backdrop, the overall aim of this study
92 was to use chlorophyll (Chl) fluorescence imaging to visually quantify differences in a range of
93 photosynthetic parameters in BSCs from the Shapotou region of the Tengger Desert, China. The objectives
94 were to: i) investigate how photosynthetic efficiency, coverage and frequency varies with light and crust
95 types; ii) characterise the relationship between photosynthetic spatial heterogeneity and distribution
96 patterns of crust photosynthetic organisms at fine spatial scales; and iii) evaluate the links between
97 photosynthetic heterogeneity and BSC succession.
98
99 **Materials and methods**
100 ***Study region and sampling***
101 In this study, BSCs were collected from the Shapotou region of Ningxia Hui Autonomous Region, located
102 on the southeastern edge of the Tengger Desert (37°32′N and 105°02′E; Fig. 1). The study region has a
103 typical continental monsoon climate, and an average elevation of 1339 m. The annual average air
104 temperature is 10.0 °C and the annual average rainfall is approximately 180 mm, falling mainly from June
105 to September, while the annual potential evapotranspiration is more than 2000 mm. The region has large
106 and dense barchan dune chains and reticulate sand dunes. The soil is mainly unconsolidated and nutrient-
107 poor sand that supports a sparse, patchy cover of vascular plants (eg. *Artemisia ordosica* and *Caragana*
108 *korshinskii*) and with BSCs covering more than 80% of soil surface (Fig. 1) [2, 10, 11].
109 Samples were collected from shrub interspaces (at least 0.2 m away from the shrub canopies) with a
110 trowel, and each type of BSCs (including the main successional stages and transitional types; Table 1) was

collected from three randomly selected sites. The minimum distance between these sites was over 50 m. At each site, all six types of BSCs were collected at least 5 m apart from each other. Care was taken to ensure the entire thickness of crusts (typically <15 mm) was sampled. All the BSCs were placed into sterilized Petri dishes, and the subsequent analysis was conducted within one month. The main dominant species in BSCs were identified under a microscope according to reference guides [31, 32], and all the analyses were repeated three times.

Chlorophyll (Chl) fluorescence imaging

To initiate photosynthetic activity all crust samples (4-5 cm^2) were rehydrated with distilled water to saturation, and then placed into a greenhouse (25 ± 2 °C) with light intensity set at 40 μE m^{-2} s^{-1} [33]. After 24 hours of photosynthetic recovery, Chl fluorescence parameters of the BSCs were imaged using an Imaging PAM (Pulse Amplitude Modulation; Mini version, Walz, Germany). Before the measurements, all BSCs were dark adapted for at least 10 minutes, then a saturating pulse (approximately 3000 μE m^{-2} s^{-1}) was supplied by the Imaging PAM to excite the crust samples. Fluorescence parameters Fo (original fluorescence) and Fm (maximal fluorescence) were automatically recorded, and Fv/Fm (the ratio of variable fluorescence to maximal fluorescence) was also calculated by the Imaging PAM. After measurement of Fv/Fm, the BSCs were illuminated with actinic light at 41, 103 and 249 μE m^{-2} s^{-1}. Under each light condition, BSCs were illuminated for at least 3 minutes, and then the saturating pulse was supplied again. During this procedure, fluorescence parameters including Yield (effective quantum yield), qP (photochemical quenching) and qN (non-photochemical quenching) were automatically recorded by the Imaging PAM. Finally, all fluorescence parameters of the different micro-regions of each BSCs were imaged and assigned different colors based on their values to facilitate effective visualization [34].

Photosynthetic coverage and frequency analysis

As an indicator of the photosynthetic activity of photosystem II (PS II), Fv/Fm represents the maximum quantum yield at which light absorbed by PS II is used for reduction of QA (primary quinone acceptor) [34-36]. In this study, crust Fv/Fm was chosen for photosynthetic coverage and frequency analysis, and was also used for the later photosynthetic spatial heterogeneity and point pattern analysis.

For photosynthetic coverage and frequency analysis, ten horizontal, equidistant parallel lines were selected from each Fv/Fm image. The coverage of excited Chl fluorescence (Fv/Fm >0.2) [28, 37] and a frequency histogram of the Fv/Fm values were calculated for each selected line. Crust photosynthetic coverage and frequency were then calculated using the selected 10 lines in the Fv/Fm image.

Photosynthetic spatial heterogeneity analysis

On each selected line on the Fv/Fm image, the photosynthetic heterogeneity index (*PHI*) was calculated using the following formula, modified according to the description in Hu and Wang [38]:

$$\sum_{i=0}^{m}\left[\sum_{j=0}^{n}\left|f(2^i, j) - M\right|/(n+1)\right]/(m+1) \qquad j + 2^i \leq N$$

where $f(2^i, j)$ is the mean of 2^i Fv/Fm values after the j_{th} Fv/Fm value, M is the mean of all the Fv/Fm values on the selected line, N is the number of Fv/Fm values on the line, and m and n are the maximum values of i and j.

For the whole crust spatial heterogeneity analysis, ten equidistant parallel lines were selected from the Fv/Fm image in the horizontal and vertical directions, respectively. Then the whole crust *PHI* index was calculated according to the *PHI* indices from each of the selected twenty lines in the Fv/Fm image. The larger the *PHI* index, the greater the photosynthetic heterogeneity of the BSCs.

155

156 ***Point pattern analysis***

157 In each crust Fv/Fm image, a 10×10 mm area of Fv/Fm values was selected to carry out the point pattern

158 analysis. All the Fv/Fm values in the two-dimensional crust image constitute a series of point events, and

159 Ripley's *K(r)* function was used to reflect the dependency of the point events in spatial pattern [39, 40]:

160 $$K(r) = \lambda^{-1} E[\#(r_{ij} \leq r)]$$

161 where λ is the density of the point events in the research area, *E* is the expectation of the point events

162 under a certain spatial scale, # is the number of point events, i and j are the two point events with the same

163 characteristics in the research area, r_{ij} represents the distance from a point to another, and *r* is the spatial

164 scale.

165 In this study, the function *L(r)* was used to estimate the distribution pattern of the point events under a

166 certain spatial scale, and was defined as follows [14, 41]:

167 $$L(r) = \sqrt{K(r)/\pi} - r$$

168 At the given spatial scale *r*, if $L(r) > 0$, the distribution of the point events represents an aggregation

169 pattern; the greater the deviation value, the higher the aggregation intensity. If $L(r) = 0$, the pattern of the

170 point events represents a random distribution, but if *L(r)* is <0, a uniform distribution would be expected

171 [14, 42].

172

173 ***Statistical Analysis and Software***

174 In this study, all the Fv/Fm values in a selected line from the crust Fv/Fm images were acquired using

175 Imaging Win software (Walz, Germany). Among the different developmental and successional BSCs, the

176 variations of each fluorescence parameter, coverage of the excited Chl fluorescence, and *PHI* index were

analyzed by One-Way ANOVA using SPSS 13.0 software (SPSS Inc., USA). In each crust type, the upper and lower envelopes in a random distribution pattern of the function *L(r)* were calculated by the Monte Carlo simulations of the null model at 99% confidence level using Programita software [14, 41]. The Monte Carlo simulation was conducted 100 times, and if the actual observed point events were higher than the upper envelope, the distribution of the point events was regarded as an aggregation pattern; on the contrary, if the actual observed point events were lower than the lower envelope, the pattern was considered to be a uniform distribution.

Results

Photosynthetic efficiency in BSCs

In this study, three main successional stages of BSCs were sampled, including cyanobacterial crusts, lichen crusts and moss crusts (Table 1). The dominant species in cyanobacterial crusts were *Microcoleus vaginatus*, while *Collema* sp. and *Bryum* sp. dominated in lichen and moss crusts, respectively (Table 1). *Microcoleus vaginatus* was found in substrate soils, and few other photosynthetic organisms were found on the surface of cyanobacterial crusts (Fig. 2A). The coverage of *Collema* sp. occupied more than 70% of the surface area of lichen crusts during dry periods, increasing up to 100% when the crust surface was moistened (Fig. 2B). *Bryum* sp. almost completely covered the surface area of moss crusts even during dry periods (Fig. 2C). Consequently, there was clear photosynthetic variation between the different successional stages of BSCs. Although the Fv/Fm values appear as blue fluorescence images in all three main successional stages (Fig. 2D, E, F), Fv/Fm increased significantly from cyanobacterial crusts to lichen crusts and to moss crusts ($P<0.05$).

Under different PAR conditions (41, 103 and 249 μE m^{-2} s^{-1}), fluorescence parameters including

Yield, qP and qN were displayed in the form of false color images (Fig. 3). With the increase in PAR, both crust Yield and qP decreased, indicated by the color changing from blue to green and purple to blue-purple, respectively. By contrast, with the increase in PAR, the color of qN changed from orange to yellow-green or yellow-green to blue-violet, although there was no statistically significant increase in the parameter value (P>0.05; Fig. S1). In addition, fluorescence parameters Yield and qP were significantly different on the different successional BSCs (P<0.05), but no significant difference was found in the fluorescence parameter qN (P>0.05; Fig. 3).

In addition to the main successional stages of BSCs, three transitional crust types were also sampled, including cyanobacteria-lichen crusts, cyanobacteria-moss crusts, and lichen-moss crusts (Fig. 4; Table 1). In cyanobacteria-lichen and cyanobacteria-moss crusts, the coverage of lichens and mosses were all <30%, while in lichen-moss crusts, the coverage of lichens and mosses was >40%, respectively (Table 1). All the transitional stage BSC Fv/Fm values were not significantly different (between 0.68 and 0.71; P>0.05; Fig. S2), and presented blue false color fluorescence images (Fig. 4), . False color images of Yield, qP and qN of the three transitional BSCs under PAR conditions of 41μE m^{-2} s^{-1} were also produced (Fig. 4). The color of Yield was blue (although numerically less than Fv/Fm), qP was purple, and qN was yellow-green (Fig. 4). There were no significant differences among the different transitional stages of BSCs (P>0.05); values were 0.63-0.66 for Yield, 0.77-0.81 for qP, and 0.19-0.36 for qN (Fig. S2).

Photosynthetic coverage and frequency in BSCs

Although all BSCs were rich in photosynthetic organisms, there were significant differences in fluorescence within the crusts (Figs. 2 and 3). The Chl fluorescence coverage was low in cyanobacterial crusts and lichen crusts, but covered almost the entire moss crusts (Figs. 3F and 5A). With the succession

of BSCs, the proportion of lichens and mosses increased gradually, and Chl fluorescence responses increased correspondingly (P<0.05; Fig. 5A). In cyanobacterial crusts, the frequency of Fv/Fm showed a unimodal pattern, and could be roughly divided into three groups: i) a no fluorescence signal group where Fv/Fm = 0 over much of the crusts; ii) a Fv/Fm value greater than 0.7 group over only a small part of the crusts; and iii) a group where the frequency of Fv/Fm values over the crust fluctuated within a small range (Fig. 6A). In lichen crusts, the frequency of Fv/Fm values showed a bimodal pattern, with peaks at Fv/Fm = 0 and 0.6-0.7 (Fig. 6B). In moss crusts, the frequency of Fv/Fm values showed a unimodal pattern with a peak of Fv/Fm greater than 0.7 (Fig. 6C). In the three transitional BSCs, the frequency of Fv/Fm values showed a similar bimodal pattern to that in lichen crusts (Fig. 6D, E, F).

Photosynthetic spatial heterogeneity and distribution pattern in BSCs

The heterogeneity of Chl fluorescence (*SHI* index) was not significantly different (P>0.05) between cyanobacterial crusts and moss crusts, but it was significantly lower in cyanobacterial and moss crusts compared to lichen crusts (P<0.05; Fig. 5B). Among the three transitional stages of BSCs, the *SHI* index of Chl fluorescence was the lowest in the cyanobacteria-lichen crusts, and similar to the indices in cyanobacterial crusts and moss crusts (P>0.05; Fig. 5B). In contrast, the spatial heterogeneity of Chl fluorescence was significantly higher in cyanobacteria-moss and lichen-moss crusts compared to the other crust types (P<0.05; Fig. 5B).

According to the observed Fv/Fm point events relative to the upper and lower envelopes of the function *L(r)*, the distribution pattern of Chl fluorescence can be clearly determined. The point pattern analysis showed that the distribution pattern of Chl fluorescence changed at different spatial scales, and also between the different crust types (Fig. 7). In cyanobacterial crusts, Chl fluorescence showed an

aggregation pattern at a spatial scale of 0-1.7 mm but a random distribution at a scale of 1.7-2.5 mm. In the other crust types, all Chl fluorescence showed an aggregation pattern at a spatial scale of 0-2.5 mm, but a tendency for a change from an aggregation to a more random distribution appeared in cyanobacteria-lichen and lichen crusts (Fig. 7).

Discussion

Light energy absorbed by Chl molecules can be used to drive photochemical reactions but alternatively can be lost as Chl fluorescence or dissipated as heat [36]. A change in Chl fluorescence is likely related to a variation of photochemical efficiency in photosynthetic organisms [26, 36]. Therefore,Chl fluorescence technology has been widely used in physiological and ecological research into cyanobacteria [33], lichens [34], higher plants [35], and also BSCs [26]. In this study, we used a Chl fluorescence imaging technique to investigate fine-scale photosynthetic spatial heterogeneity in different BSCs types, in order to provide more information on crust photosynthetic mechanisms.

Imaging photosynthetic efficiency variation in BSCs

Imaging PAM presents Chl fluorescence signals in the form of a false color image, which reflects the photosynthetic heterogeneity and distribution pattern in BSCs. The composition of photosynthetic organisms changes with the succession of BSCs [8, 43], thus leading to distinctive imaging of Chl fluorescence signals excited from different crust types (Figs. 2 and 4). Compared with other Chl fluorescence detectors (such as Plant Efficiency Analyzer; PEA), imaging Chl fluorescence using Imaging PAM can show photosynthetic activity in BSCs in greater detail at finer scales. This helps improve our understanding of the fine scale distribution and functions of BSCs. In our study region the basic spatial

elements (photoautotrophic organisms) are cyanobacteria, lichens and mosses. Therefore, we can regard the whole region BSCs as comprising three different types, dominated by cyanobacteria, lichens or mosses, respectively.

Photosynthetic performance at fine scales is reflected by the adaptation of PS II of the photosynthetic organisms residing in BSCs. The Fv/Fm ratio reflects the largest solar energy conversion efficiency in the PS II reaction center, and is expected to decrease under environmental stresses such as dessication [26, 34]. However, in unstressed conditions (e.g. when crusts are hydrated), Fv/Fm is maintained at a relatively stable level. Furthermore, our results reveal that the Fv/Fm gradually increased with the succession from cyanobacterial crusts to lichen crusts and to moss crusts ($P<0.05$), which indicates that the maximum photosynthetic efficiency is higher in the later successional BSCs. Under a given light condition, Yield reflects the effective photosynthetic efficiency (quantum yield) of PS II when parts of the PS II reaction centers are closed [34, 36]. Therefore, Yield was lower than Fv/Fm, and decreased gradually with increasing PAR (Fig. 3). Similarly, qP also decreased with increasing PAR (although the decrease in cyanobacterial crusts was not statistically significant; $P>0.05$), reflecting a decrease in the ratio of open PS II centers. With decreases of Yield and qP, the non-photochemical quenching parameter qN was expected to increase, so that more light energy could be quenched in non-photochemical form. This is because when PAR is within a certain range, BSCs can maintain the stability of qP by increasing qN [36, 45]. However, in our study, as PAR increased from 41 to 249 μE m^{-2} s^{-1}, the increase of qN was still limited. Similar to Fv/Fm, Yield and qP also gradually increased with the crust succession, although no significant difference was found in the fluorescence parameter qN. This is further evidence that photosynthetic efficiency is stronger in the later successional BSCs.

Photosynthetic spatial heterogeneity in BSCs

Although a variety of fluorescence parameters were measured in our study, in reality all the fluorescence parameters were excited from the same photosynthetic organisms in each BSCs, so that all the fluorescence parameters exhibited the same spatial distribution characteristics. In the present study, Fv/Fm was used to characterise the photosynthetic heterogeneity and spatial distribution pattern. In cyanobacterial crusts, photosynthetic spatial heterogeneity may be affected by the uneven distribution of cyanobacterial filaments not only on the surface but also at depth because most cyanobacteria reside in the surface substrate (the exception being some species with strong radiation-protective ability, such as *Scytonema* and *Nostoc*) [4, 5]. The incident light in such crusts is rapidly attenuated by the soil particles and exopolymeric matrix before it excites the cyanobacteria [23, 44]; in turn, the excited fluorescence signals are similarly attenuated before they can be detected by the Imaging PAM, which eventually leads to the low photosynthetic fluorescence coverage and unimodal pattern of Fv/Fm = 0 in cyanobacterial crusts (Figs. 5A and 6A).

As BSCs succeed, the position of dominant photosynthetic organisms changes from the substrate to the surface. Lichens are the symbionts of cyanobacteria (or algae in some lichens) and fungi, so the Chl fluorescence signals of lichen crusts in reality were excited from the symbiotic cyanobacteria. These cyanobacteria are covered by fungi and also large quantities of exopolymeric matrix, so most symbiotic cyanobacteria in the lichen crusts are not directly exposed to the air [46], which leads to significant attenuation of incident light. Similarly, the fluorescence signals excited from the symbiotic cyanobacteria by the attenuated incident light are further attenuated before the Imaging PAM can detect them. In our study, no fluorescence signal was excited in most micro-regions of lichen crusts (Fig. 5A). However, the frequency of Fv/Fm with high values (>0.6) was significantly higher than the frequency with other values

(except Fv/Fm = 0) in lichen crusts, and thus the frequency of Fv/Fm was bimodal (Fig. 6B).

In moss crusts, mosses are not only directly distributed on the crust surface, but also directly accept incident light and the excited fluorescence signals could be directly detected by the Imaging PAM. Therefore, the excited fluorescence covered almost the entire moss crusts, and most of the Fv/Fm values were high (>0.6) and unimodal (Fig. 6C).

In summary, the heterogeneity of Chl fluorescence can be attributed to the heterogeneous distribution of photosynthetic organisms in BSCs, which also reflects differences in successional stage of BSCs in different micro-regions. In the present study, the photosynthetic heterogeneity index *PHI* ranged from 0.02 to 0.17 among the different BSC types, with the highest values in cyanobacteria-moss and lichen-moss crusts (Fig. 5B).

Photosynthetic spatial scale associated with crust succession

Our results confirm that crust heterogeneity is a common phenomenon, and that it varies with spatial scale. In cyanobacterial crusts, the results suggested cyanobacterial distribution changed from aggregation to random with the increasing spatial scale; while in lichen and moss crusts, all the photosynthetic organisms aggregated throughout the experimental spatial scale (0-2.5 mm), although there was a tendency for a change to a more random distribution pattern in lichen crusts (Fig. 7B). However, due to the size limitations of the mini Imaging PAM used in this study, the spatial scale was limited in 2.5 mm, so it is not clear if the tendency towards a random distribution persisted as spatial scale increased. Using the Max version of Imaging PAM or other equipment will help us understand the heterogeneous distribution of BSCs in even greater detail and provide more direct evidence of the heterogeneous distribution of BSCs at larger scales.

There are parallels between the controls over small-scale photosynthetic heterogeneity within BSCs and variations in BSCs cover over larger regions where water availability, effective incidence of light under micro-topography and other physicochemical conditions affect crust distribution [6, 19-21]. Together, variations at all scales add spatial heterogeneity and ecological diversity to the landscape. Chl fluorescence technology can not only detect the landscape-scale distribution of photosynthetic organisms and the associated spatial heterogeneity, but also provides a useful approach for monitoring environmental conditions and diagnosing photosynthetic change [47], which ultimately may inform the maintenance and management of healthy BSCs. Using Chl fluorescence technology in field settings removes the need for crust destruction, and also provides a good proxy for Chl-a content [26]. Furthermore, the present study reveals that Chl fluorescence imaging can clearly provide a more accurate indication about crust succession at a fine scale.

The results presented in this study and published elsewhere (e.g. [26, 48]) all support the idea that later successional BSCs have higher photosynthetic efficiency than earlier stages, and are likely to have a greater range of ecological functions (e.g. carbon and nitrogen fixation). Various techniques could therefore be used to accelerate the succession of BSCs in a bid to mitigate against a range of land degradation processes [3, 18, 49, 50]. For example, a large scale, straw checkerboard technique was used successfully in the study region from 1956 to promote the development and succession of BSCs [51]. Measures are also needed to ensure that BSCs are not overly disturbed (e.g. by maintaining well managed grazing regimes) [52], because disturbance could convert later to early successional BSCs, thus representing a significant loss of photosynthetic carbon fixation and other relevant ecological functions [22, 48].

Conclusion

In this study, a novel Chl fluorescence imaging technique was used to investigate the photosynthetic heterogeneity of different crust types found in the Tengger Desert, China. The results show that with crust succession, maximum photosynthetic efficiency (Fv/Fm after dark adaptation) gradually increased, and fluorescence coverage also increased correspondingly. Under light conditions, although effective photosynthetic efficiency decreased with the increasing PAR, it increased with crust succession. Cyanobacterial crusts and moss crusts showed the two extremes of photosynthetic coverage, being mostly low and mostly high, respectively, but both displayed the same unimodal Fv/Fm frequency. The heterogeneity (*SHI* index) was not significantly different ($P > 0.05$) between cyanobacterial and moss crusts but was higher in lichen crusts ($P < 0.05$), which had a bimodal pattern of Fv/Fm frequency. Point pattern analysis showed that distribution patterns of Chl fluorescence varied at different spatial scales and among the different crust types. This implies that when assessing crust photosynthetic performance, such as its role in carbon fixation and storage, in addition to consideration of BSC succession, it is still necessary to consider the impact of scale, particularly the heterogeneity of BSCs. In-depth understanding of the characteristics of photosynthetic heterogeneity and the complexity of landscapes at different scales will provide further insights into crust development and succession, and enable more accurate assessment of photosynthetic carbon fixation, storage and other ecological functions through the up-scaling of heterogeneous ground-based data.

Acknowledgements

This study was kindly supported by the Strategic Priority Research Program of the Chinese Academy of Sciences (No. XDA17010502), National Natural Science Foundation of china (Nos. 31670456 and

31300322), Youth Innovation Promotion Association CAS (No. 2017385) and European Union's Horizon 2020 research and innovation programme under the Marie Skłodowska-Curie Grant (No. 663830). The paper was prepared while S. Lan was a Sêr Cymru Fellow at Aberystwyth University, and L. Wu was a Visiting Scholar at Aberystwyth University.

References

1. Hu C, Gao K, Whitton, BA (2012) Semi-arid Regions and Deserts. In: Whitton, B.A., Ed. Ecology of Cyanobacteria II: Their Diversity in Space and Time. Springer Science+Business Media, Dordrecht, pp 345-369.
2. Lan S, Wu L, Zhang D, Hu C (2015) Analysis of environmental factors determining development and succession in biological soil crusts. Sci Total Environ 538:492-499.
3. Hu C, Liu Y, Song L, Zhang D (2002) Effect of desert soil algae on the stabilization of fine sands. J Appl Phycol 14:281-292.
4. Lan S, Wu L, Zhang D, Hu C (2012) Successional stages of biological soil crusts and their microstructure variability in Shapotou region (China). Environ Earth Sci 65(1):77-88.
5. Hu C, Zhang D, Huang Z, Liu Y (2003) The vertical microdistribution of cyanobacteria and green algae within desert crusts and the development of the algal crusts. Plant Soil 257 :97-111.
6. Lan S, Zhang Q, Wu L, Liu Y, Zhang D, Hu C (2014) Artificially Accelerating the Reversal of Desertification: Cyanobacterial Inoculation Facilitates the Succession of Vegetation Communities. Environ Sci Technol 48:307-315.
7. Belnap J, Gillette DA (1998) Vulnerability of desert biological soil crusts to wind erosion: the influences of crust development, soil texture, and disturbance. J Arid Environ 39(2):133-142.

8. Elliott DR, Thomas AD, Hoon SR, Sen R (2014) Niche partitioning of bacterial communities in biological crusts and soils under grasses, shrubs and trees in the Kalahari. Biodivers Conserv 23:1709-1733.
9. Eldridge DJ, Zaady E, Shachak M (2000) Infiltration through three contrasting biological soil crusts in patterned landscapes in the Negev, Israel. Catena 40:323-336.
10. Lan S, Hu C, Rao B, Wu L, Zhang D, Liu Y (2010) Non-rainfall water sources in the topsoil and their changes during formation of man-made algal crusts at the eastern edge of Qubqi Desert, Inner Mongolia. Sci China Life Sci 53:1135-1141.
11. Li X, Jia X, Long L, Zerbe S (2005) Effects of biological soil crusts on seed bank, germination and establishment of two annual plant species in the Tengger Desert (N China). Plant Soil 277:375-385.
12. Li X, Jia R, Chen Y, Huang L, Zhang P (2011) Association of ant nests with successional stages of biological soil crusts in the Tengger Desert, Northern China. Appl Soil Ecol 47:59-66.
13. Pickett STA, Cadenasso ML (1995) Landscape ecology: Spatial heterogeneity in ecological systems. Science 269:331-334.
14. Wiegand T, Moloney KA (2004) Rings, circles and null-models for point pattern analysis in ecology. Oikos 104:209-229.
15. Shen G, He F, Waagepetersen R, Sun I, Hao Z, Chen Z, Yu M (2013) Quantifying effects of habitat heterogeneity and other clustering processes on spatial distributions of tree species. Ecology 94(11):2436-2443.
16. Bowker MA, Belnap J, Davidson DW, Goldstein H (2006) Correlates of biological soil crust abundance across a continuum of spatial scales: Support for a hierarchical concep tualmodel. J Appl Ecol 43 :152-163.

17. Baillod AB, Tscharntke T, Clough Y, Batáry P (2017) Landscape-scale interactions of spatial and temporal cropland heterogeneity drive biological control of cereal aphids. J Appl Ecol 54:1804-1813.
18. Liu Y, Cockell CS, Wang G, Hu C, Chen L, De Philippis R (2008) Control of Lunar and Martian Dust-Experimental Insights from Artificial and Natural Cyanobacterial and Algal Crusts in the Desert of Inner Mongolia, China. Astrobiology 8 :75-86.
19. Zaady E, Kuhn U, Wilske B, Sandoval-Soto L, Kesselmeier J (2000) Patterns of CO_2 exchange in biological soil crusts of successional age. Soil Biol Biochem 32:959-966.
20. Zaady E, Karnieli A, Shachak M (2007) Applying a field spectroscopy technique for assessing successional trends of biological soil crusts in a semi-arid environment. J Arid Environ 70:463-477.
21. Kidron GJ, Vonshak A, Abeliovich A (2008) Recovery rates of microbiotic crusts within a dune ecosystem in the Negev Desert. Geomorphology 100:444-452.
22. Viles HA (2008) Understanding dryland landscape dynamics: do biological crusts hold the key? Geography Compass 2(3):899-919.
23. Garcia-Pichel F, Belnap J (1996) Microenvironments and microscale productivity of cyanobacterial desert crusts. J Phycol 32:774-782.
24. Bowker MA, Belnap J, Davidson DW, Phillips SL (2005) Evidence for micronutrient limitation of biological soil crusts: Importance to arid-lands restoration. Ecol Appl 15:1941-1951.
25. Abed RMM, Lam P, De Beer D, Stief P (2013) High rates of denitrification and nitrous oxide emission in arid biological soil crusts from the Sultanate of Oman. ISME J 7:1862-1875.
26. Lan S, Wu L, Zhang D, Hu C (2017) Biological soil crust community types differ in photosynthetic pigment composition, fluorescence and carbon fixation in Shapotou region of China. Appl Soil Ecol 111:9-16.

441 27. Wu L, Lan S, Zhang D, Hu C (2011) Small-scale Vertical Distribution of Algae and Structure of Lichen
442 Soil Crusts. Microbial Ecol 62:715-724.
443 28. Wu L, Lan S, Zhang D, Hu C (2013) Functional reactivation of photosystem II in lichen soil crusts
444 after long-term desiccation. Plant Soil 369:177-186
445 29. Swap RJ, Annegarn HJ, Suttles JT, et al (2002) The Southern African Regional Science Initiative
446 (SAFARI 2000): Overview of the Dry Season Field Campaign. S Afr J Sci 98(3):125-130.
447 30. Dean WRJ, Milton SJ, Jeltsch F (1999) Large trees, fertile islands, and birds in arid savanna. J Arid
448 Environ 41:61-78.
449 31. Hu H, Li R, Wei Y, Zhu H, Chen J, Shi Z (1980) Freshwater Algae in China. Shanghai Science and
450 Technology Press, Shanghai (in Chinese).
451 32. Rosentreter R, Bowker M, Belnap J (2007) A Field Guide to Biological Soil Crusts of Western U.S.
452 Drylands. U.S. Government Printing Office, Denver
453 33. Ohad I, Raanan H, Keren N, Tchernov D, Kaplan A (2010) Light-induced changes within photosystem
454 II protects *Microcoleus* sp. in biological desert sand crusts against excess light. PLoS ONE 5(6):e11000.
455 34. Wu L, Lei Y, Lan S, Hu C (2017) Photosynthetic recovery and acclimation to excess light intensity in
456 the rehydrated lichen soil crusts. PLoS ONE 12(3):e0172537.
457 35. Heber U, Bilger W, Shuvalov VA (2006) Thermal energy dissipation in reaction centres and in the
458 antenna of photosystem II protects desiccated poikilohydric mosses against photo-oxidation. J Exp Bot
459 57:2993-3006.
460 36. Baker NR (2008) Chlorophyll fluorescence: a probe of photosynthesis in vivo. Annu Rev Plant Biol
461 59:89-113.
462 37. Green TGA, Schlensog M, Sancho LG, Winkler JB, Broom FD, Schroeter B (2002) The photobiont

463 determines the pattern of photosynthetic activity within a single lichen thallus containing
464 cyanobacterial and green algal sectors (photosymbiodeme). Oecologia 130:191-198.
465 38. Hu H, Wang X (2008) Unified index to quantifying heterogeneity of complex networks. Physica A
466 387(14):3769-3780.
467 39. Ripley BD (1976) The second-order analysis of stationary point processes. J Appl Probab 13:255-266.
468 40. Shi P, Ge F, Yang Q, Wang J (2009) A new algorithm of the edge correction in the point pattern
469 analysis and its application. Acta Ecologica Sinica 29(2) :804-809.
470 41. Wiegand T, Moloney KA (2014) A handbook of spatial point pattern analysis in ecology. Chapman and
471 Hall/CRC press, Boca Raton, FL.
472 42. Law R, Illian J, Burslem DFRP, Gratzer G, Gunatilleke CVS, Gunatilleke IAUN (2009) Ecological
473 information from spatial patterns of plants: insights from point process theory. J Ecol 97:616-628.
474 43. Lan S, Wu L, Zhang D, Hu C (2013) Assessing Level of Development and Successional Stages in
475 Biological Soil Crusts with Biological Indicators. Microbial Ecol 66:394-403.
476 44. Mugnai G, Rossi F, Felde VJ, Colesie C, Büdel B, Peth S, Kaplan A, De Philippis R (2018).
477 Development of the polysaccharidic matrix in biocrusts induced by a cyanobacterium inoculated in
478 sand microcosms. Biol Fert Soils 54:27-40.
479 45. Müller P, Li X, Niyogi KK (2001) Non-Photochemical Quenching. A Response to Excess Light Energy.
480 Plant Physiol 125:1558-1566.
481 46. Wu L, Zhang G, Lan S, Zhang D, Hu C (2013) Microstructures and photosynthetic diurnal changes in
482 the different types of lichen soil crusts. Eur J Soil Biol 59:48-53.
483 47. Lan S, Wu L, Zhang D, Hu C (2012) Composition of photosynthetic organisms and diurnal changes of
484 photosynthetic efficiency in algae and moss crusts. Plant Soil 351:325-336.

48. Housman DC, Powers HH, Collins AD, Belnap J (2006) Carbon and nitrogen fixation differ between successional stages of biological soil crusts in the Colorado Plateau and Chihuahuan Desert. J Arid Environ 66:620-634.
49. Bowker MA, Reed SC, Belnap J, Phillips SL (2002) Temporal variation in community composition, pigmentation, and Fv/Fm of desert cyanobacterial soil crusts. Microbial Ecol 43:13-25.
50. Belnap J (1993) Recovery rates of cryptobiotic crusts: Inoculant use and assessment methods. Great Basin Nat 53:89-95.
51. Li X, Xiao H, He M, Zhang J (2006) Sand barriers of straw checkerboards for habitat restoration in extremely arid desert regions. Ecol Eng 28:149-157.
52. Thomas AD (2012) Impact of grazing intensity on seasonal variations in SOC and soil CO_2 efflux in two semiarid grasslands in southern Botswana. Philos T Roy Soc B 367:3076-3086.

Figure captions:

Fig. 1 Location of the study region (left) and example of the characteristic patches of vascular plants and BSCs on the Tengger Desert margins in the Shapotou region (right).

Fig. 2 The three main successional stages of BSCs in the Shapotou region, including cyanobacterial crusts (A), lichen crusts (B) and moss crusts (C), and their fluorescence images (Fv/Fm) in (D), (E), (F), respectively. The images are in false color, and the color scale on each Fv/Fm image represents the values from 0 (red) to 1 (purple).

Fig. 3 Comparison of fluorescence parameters Yield, qP and qN in the three main successional stages of BSCs. (A), (B) and (C) show the comparison of the values of three parameters under different PAR conditions; for a given PAR condition, values with different letters indicate that the difference is significant at the 0.05 level (P<0.05). Cyanobacterial crusts (D), lichen crusts (E) and moss crusts (F) show the fluorescence images of three parameters under different PAR conditions (from left to right, 41, 103 and 249 μE m^{-2} s^{-1}). The images in (D), (E) and (F) are in false color, and the color scale on each image represents the values from 0 (red) to 1 (purple).

Fig. 4 Three transitional stages of BSCs in the Shapotou region, including cyanobacteria-lichen crusts (A), cyanobacteria-moss crusts (B) and lichen-moss crusts (C), and their fluorescence images including Fv/Fm, Yield, qP and qN. The Yield, qP and qN were determined under the PAR condition of 41 μE m^{-2} s^{-1}. The images are in false color, and the color scale on each image represents the values from 0 (red) to 1 (purple).

Fig. 5 Box and whisker plots of fluorescence coverage (A) and spatial heterogeneity index (B) in the different successional stages of BSCs (see Table 1 for the definition of abbreviations). For each parameter, the values with different letters indicate that the difference is significant at the 0.05 level (P<0.05).

Fig. 6 Frequency histogram of Fv/Fm intervals in the different successional stages of BSCs, including

cyanobacterial crusts (A), lichen crusts (B), moss crusts (C), cyanobacteria-lichen crusts (D), cyanobacteria-moss crusts (E) and lichen-moss crusts (F).

Fig. 7 Point pattern analysis of Chl fluorescence in the different successional stages of BSCs, including cyanobacterial crusts (A), lichen crusts (B), moss crusts (C), cyanobacteria-lichen crusts (D), cyanobacteria-moss crusts (E) and lichen-moss crusts (F). The solid and dotted lines in the figure show the envelopes in the random distribution pattern of the function *L(r)* and the observed fluorescence values, respectively.

Fig. 1

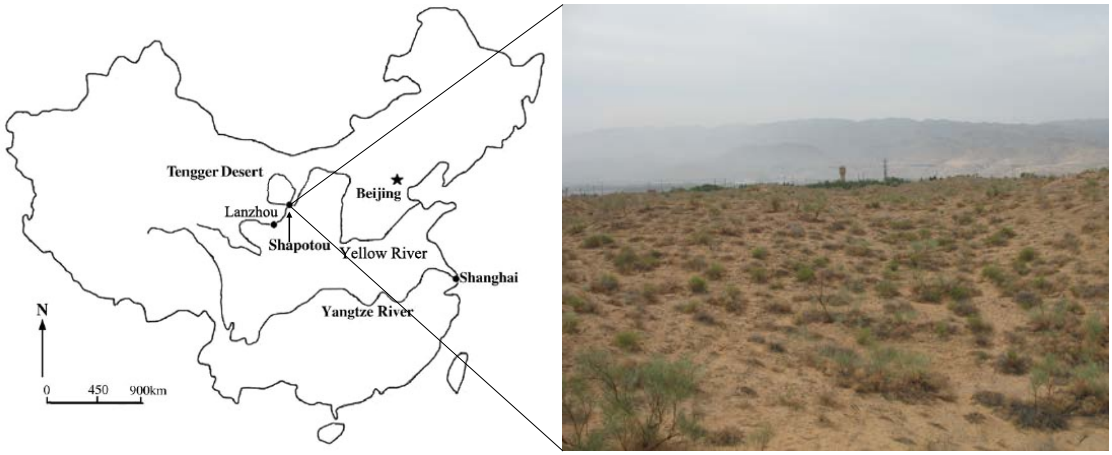
Tengger Desert
Beijing
Lanzhou
Shapotou
Yellow River
Shanghai
Yangtze River
N
0 450 900km

Fig. 2

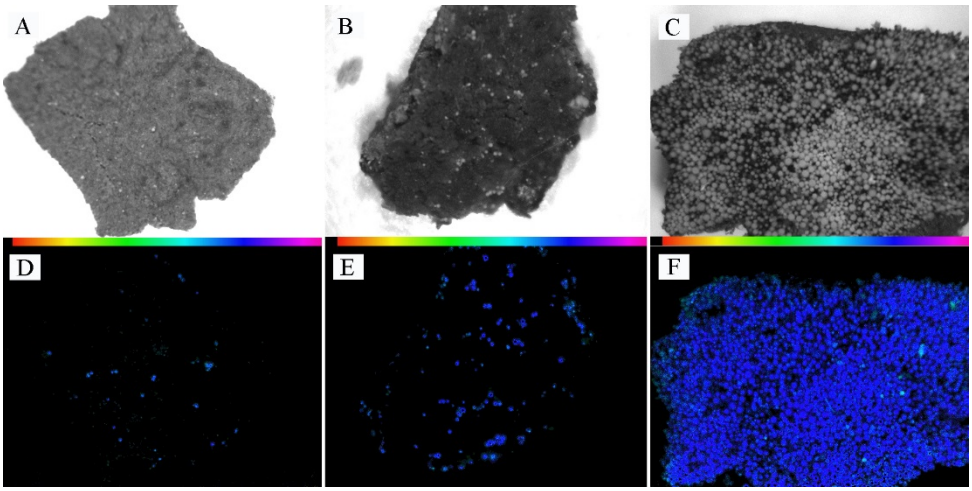

603 **Fig. 3**

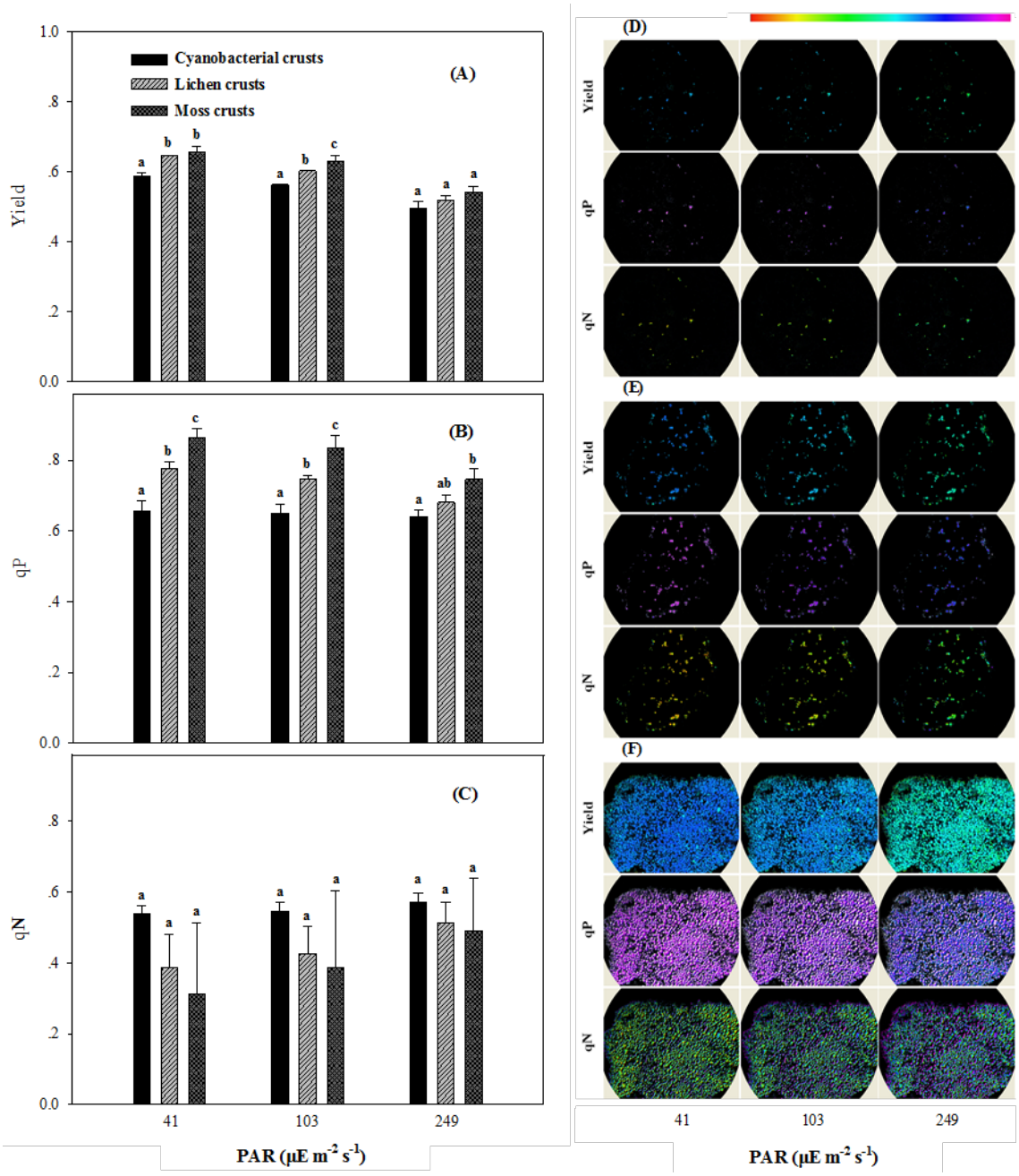

604

605

606

607

608

609

610

611

612 **Fig. 4**

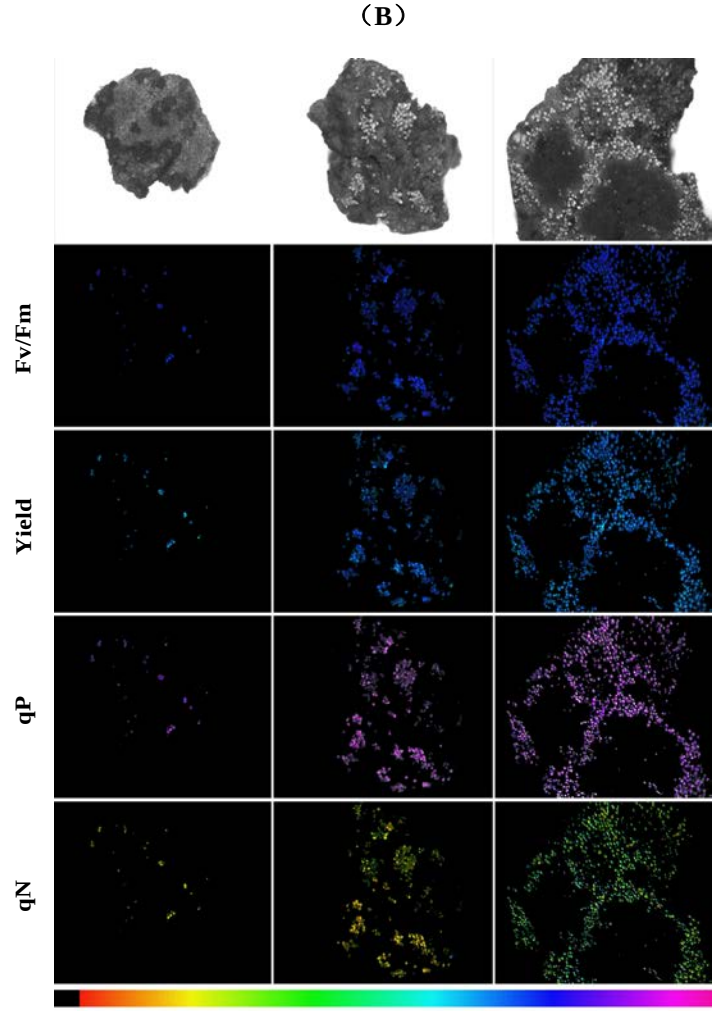

613

614

615

616

617

618

619

620

621

622

623

624

625

Fig. 5

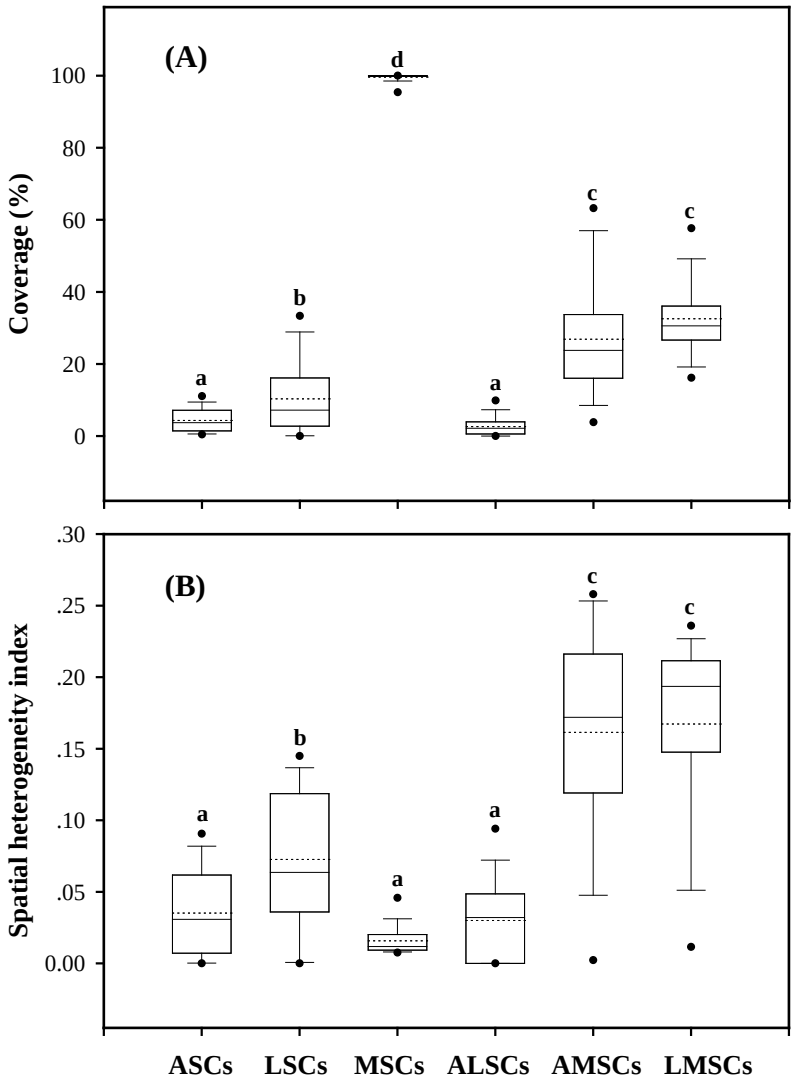
(A)
Coverage (%)
100
80
60
40
20
0
a
b
d
a
c
c
(B)
Spatial heterogeneity index
.30
.25
.20
.15
.10
.05
0.00
a
b
a
a
c
c
ASCs
LSCs
MSCs
ALSCs
AMSCs
LMSCs

Fig. 6

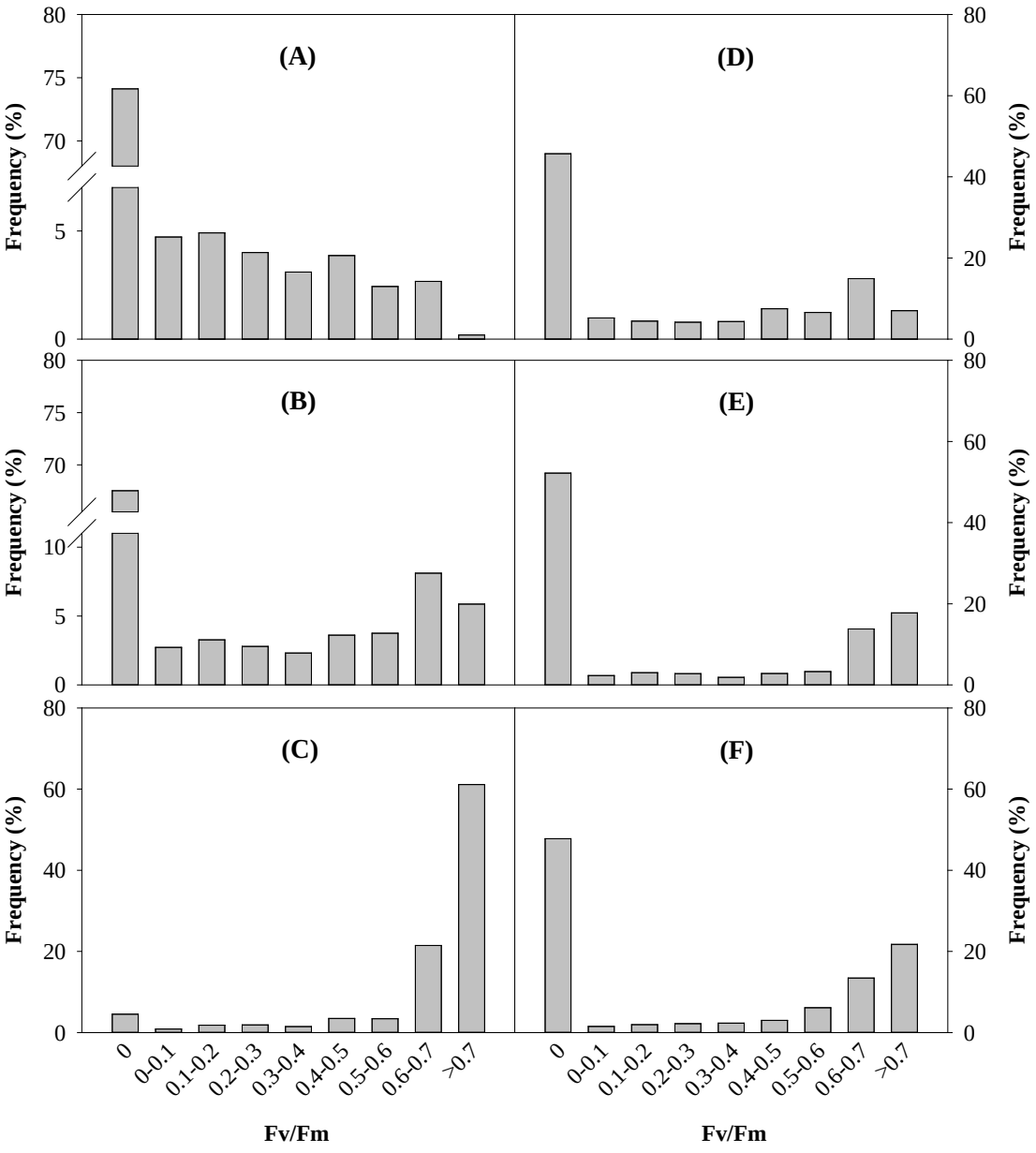

Fig. 7

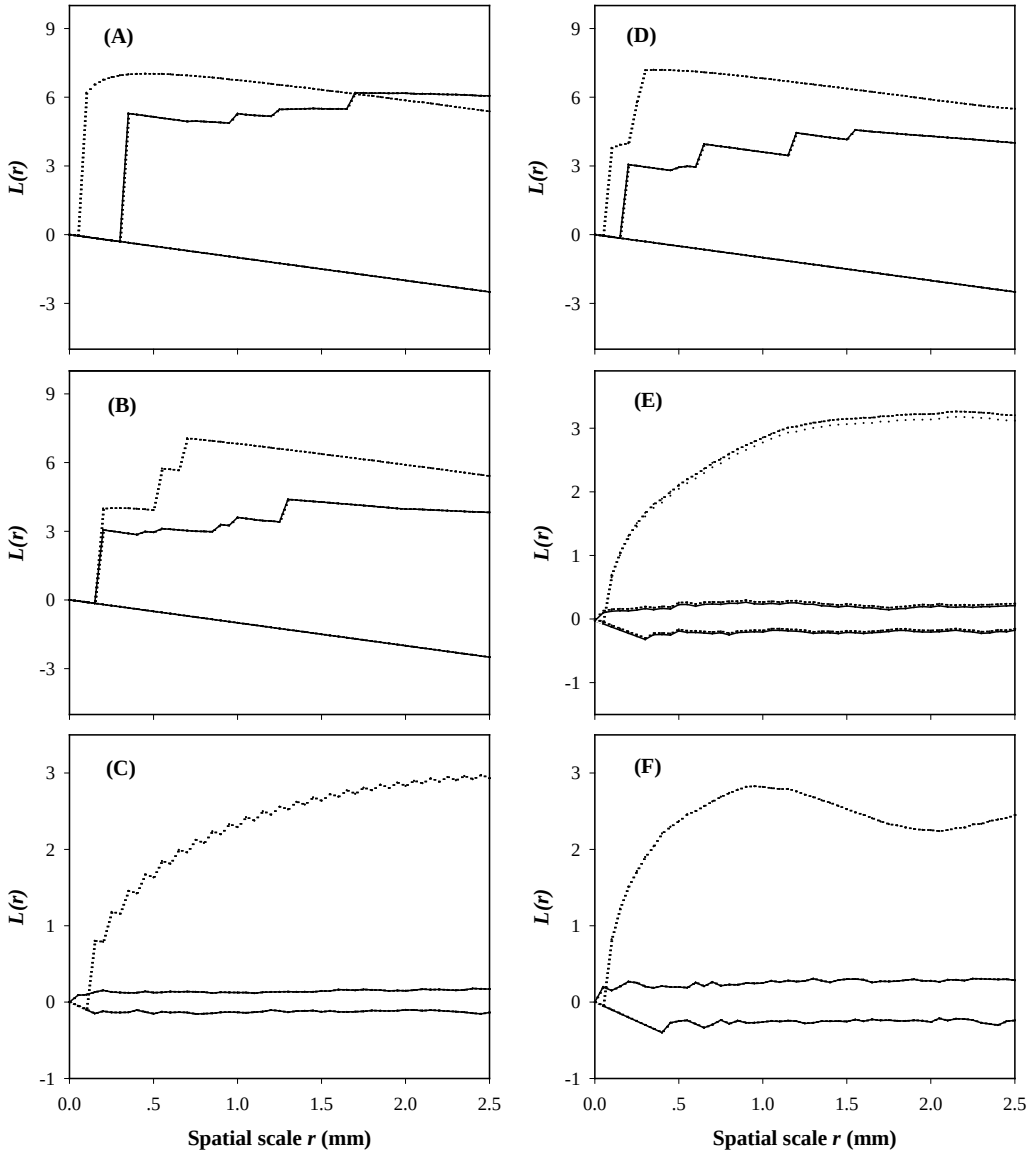

662 Table 1 Characteristics of the different successional stages of BSCs in the Shapotou region

Abbreviations	Crust successional stages	Dominant organisms	Crust color	Crust thickness (mm)	Cyanobacterial coverage (%)	Lichen coverage (%)	Moss coverage (%)
CSCs	Cyanobacterial (soil) crusts	*Microcoleus vaginatus*	Gray	2.93 ± 0.13	>97	0	<3
LSCs	Lichen (soil) crusts	*Collema* sp. (cyanolichen)	Black	7.44 ± 1.51	<27	>70	<3
MSCs	Moss (soil) crusts	*Bryum* sp.	Brown	14.62 ± 1.77	0	0	100
CLSCs	Cyanobacteria-lichen (soil) crusts	*M. vaginatus* and *Collema* sp.	Gray and black	5.72 ± 1.24	>67	<30	<3
CMSCs	Cyanobacteria-moss (soil) crusts	*M. vaginatus* and *Bryum* sp.	Gray and brown	6.18 ± 0.93	>70	0	<30
LMSCs	Lichen-moss (soil) crusts	*Collema* sp. and *Bryum* sp.	Black and brown	10.54 ± 1.18	<10	>40	<50

663

664

665

666

667

668

669

670

671

672

673

674

675

676

677

678

679

680

681

682

Supplementary Material for:

Small-scale spatial heterogeneity of photosynthetic fluorescence in biological soil crusts

Shubin Lan, Andrew David Thomas, Stephen Tooth, Li Wu, Chunxiang Hu*

* Corresponding author: Tel/Fax.: +86 27 68780866; E-mail address: cxhu@ihb.ac.cn

This supplementary file includes 3 pages of information:

Number of figures: 2

Fig. S1 Comparison of three fluorescence parameters Yield (A), qP (B) and qN (C) under different actinic light conditions. For a crust sample, the values with different letters indicate the difference is significant at 0.05 level (P<0.05).

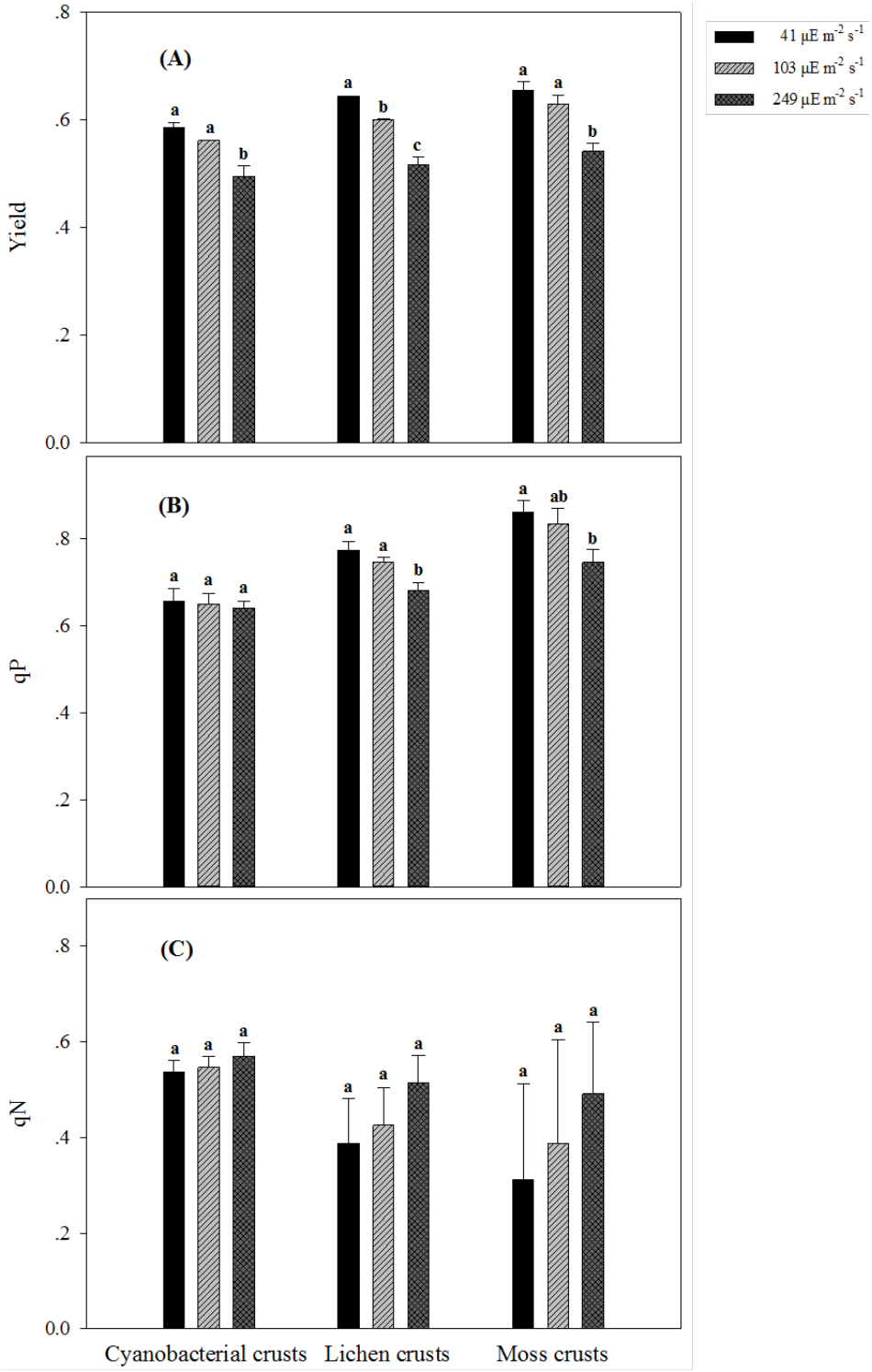

Fig. S2 Comparison of fluorescence parameters Fv/Fm after dark adaptation and Yield, qP, qN under the light condition of 41μE m^{-2} s^{-1}. For each parameter, the values with same letters indicate the difference is not significant at 0.05 level (P>0.05).